

NEW GEOEFFECTIVE PARAMETERS OF VERY FAST HALO CORONAL MASS EJECTIONS

Y.-J. MOON,¹ K.-S. CHO,¹ M. DRYER,^{2,3} Y.-H. KIM,¹ SU-CHAN BONG,¹ JONGCHUL CHAE,⁴ AND Y. D. PARK^{1,5}

Received 2004 October 31; accepted 2005 January 13

ABSTRACT

We have examined the physical characteristics of very fast coronal mass ejections (CMEs) and their geoeffective parameters. For this we consider *SOHO* LASCO CMEs whose speeds are larger than 1300 km s^{-1} . By examining all *SOHO* EIT and *SOHO* LASCO images of the CMEs, we selected 38 front-side very fast CMEs and then examined their associations with solar activity such as X-ray flares and type II bursts. As a result, we found that among these front-side fast CMEs, 25 are halo (or full halo) CMEs with span of 360° , 12 are partial halo CMEs with span greater than 130° , and only one is a broadside CME, with a span of 53° . There are 13 events that are shock-deflected CMEs: six are full halo CMEs, and seven are partial halo CMEs. It is found that about 60% (23/38) CMEs were ejected from the western hemisphere. We also note that these very fast CMEs have very high associations with other solar activities: all the CMEs are associated with X-ray flares (X-12, M-23, C-3), and about 80% of the CMEs (33/38) were accompanied by type II bursts. For the examination of CME geoeffectiveness, we select 12 halo CMEs whose longitudes are less than 40° , which are thought to be the most plausible candidates of geoeffective CMEs. Then we examine the relation between their CME physical parameters (mass, column density, location of an associated flare, and direction) and the Dst index. In particular, a CME direction parameter, which is defined as the maximum ratio of its shorter front from solar disk center and its longer one, is proposed as a new geoeffective parameter. Its major advantage is that it can be directly estimated from coronagraph observation. It is found that while the location of the associated flare has a poor correlation with the Dst index, the new direction parameter has a relatively good correlation. In addition, the column density of a CME also has a comparable good correlation with the Dst index. Noting that the CME column density is strongly affected by the direction of a CME, our results imply that the CME direction seems to be the most important parameter that controls the geoeffectiveness of very fast halo CMEs.

Subject headings: solar-terrestrial relations — Sun: coronal mass ejections (CMEs) — Sun: flares

1. INTRODUCTION

During the past several decades, coronal mass ejections (CMEs) have emerged as one of the main solar activities, since they are thought to be main geoeffective objects that produce geomagnetic storms. The complex family of CMEs, sometimes with their leading shock waves, has been called interplanetary coronal mass ejections (ICMEs) during their heliospheric propagation. The specific case of fast steady flow–slow transient flow interaction was studied by Zhao (1992), who first coined the term ICME. It was also used to refer to the more general case (Dryer 1994) without knowledge of the acronym's previous use.

Their near-Sun kinematic characteristics have been well studied by several coronagraphs. MacQueen & Fisher (1983) suggested that CMEs be classified into two types by analyzing the height-speed plots of 12 looplike CMEs observed with the Mauna Loa K-coronameter covering $1.2\text{--}2.4 R_\odot$. In their study, flare-associated CMEs showed higher speeds and small accelerations, whereas eruptive-filament-associated CMEs exhibited lower speeds and large accelerations. This argument has been supported by several subsequent observational studies (St. Cyr et al. 1999; Sheeley et al. 1999; Andrews & Howard 2001; Moon et al. 2002), although there are some counterexamples (Moon

et al. 2004). According to these studies, the speed of a CME ranges from below 100 to about 2500 km s^{-1} (e.g., St. Cyr et al. 1999; Moon et al. 2002). Specifically, Moon et al. (2002) presented a comprehensive statistical study on CME kinematics of *SOHO* LASCO CMEs from 1996 to 2000. According to their study, the mean CME speed is about 477 km s^{-1} for all CMEs, 534 km s^{-1} for CMEs associated with flares greater than C1 class, and 684 km s^{-1} for CMEs associated with flares greater than M1 class (for details, see Table 1 of their paper). Recently, Andrews (2003) also showed that large flares were much more likely to be associated with fast CMEs. While there have been a few studies on the physical characteristics of individual very fast CMEs, e.g., rapid accelerations (Gallagher et al. 2003), far-ultraviolet spectroscopic observations (Raymond et al. 2003), and radio signatures (Maia et al. 1999), their physical characteristics and their association with other solar activities in terms of statistics have never been examined. In this paper we examine the physical characteristics of very fast CMEs as an extreme case of CME kinematics. For this, we consider very fast front-side CMEs whose plane-of-sky speeds in the LASCO field of view are larger than 1300 km s^{-1} , which is comparable to the sum of mean speed and 3 times the standard deviation of all CME speeds (Moon et al. 2002). We investigate their physical characteristics as well as their associations with solar activities such as solar flares and type II bursts.

To examine the geoeffectiveness of the very fast CMEs, we first select front-side halo CMEs, since they are thought to be good potential candidates that can produce strong geomagnetic storms (e.g., Wang et al. 2002; Zhang et al. 2003; Zhao & Webb 2003). In addition, we note that not all of these CMEs are geoeffective; that is, a prediction based only on the front-side halo CMEs may produce many false alarms (St. Cyr et al. 2000).

¹ Korea Astronomy and Space Science Institute, Whaamdong, Yooseong-ku, Daejeon, 305-348, Korea; yjmoon@kasi.re.kr.

² NOAA Space Environment Center, 325 Broadway, Boulder, CO 80303.

³ Exploration Physics International, Inc., Huntsville, AL 35806.

⁴ Astronomy Program, School of Earth and Environmental Sciences, Seoul National University, 151-742, Korea.

⁵ Big Bear Solar Observatory, NJIT, 40386 North Shore Lane, Big Bear City, CA 92314.

TABLE 1
PHYSICAL CHARACTERISTICS OF VERY FAST CORONAL MASS EJECTIONS

Date	Time ^a	Width (deg)	V_c^b (km s ⁻¹)	A_c^c (m s ⁻²)	Flare Start	X-Ray Class	Position (deg)	AR No.	Magnitude Class	Type II	Shock Deflection
1997 Nov 6.....	12:10	Halo	1556	-44	11:49	X9.4	S18, W63	8100	$\beta\gamma$	11:53	No
1998 Apr 27.....	08:56	Halo	1385	74	08:55	X1.0	S16, E50	8210	$\beta\delta$	09:08	No
1998 Apr 29.....	16:58	Halo	1374	-44	16:06	M6.8	S18, E20	8210	$\beta\gamma$	16:22	No
1998 May 9.....	03:35	178	2331	-140	03:04	M7.7	N28, W63	8214	β	03:26	No
1998 Dec 18.....	18:09	Halo	1749	17	17:13	M8.0	N19, E64	8415	β	17:27	No
1999 May 3.....	06:06	Halo	1584	15	05:36	M4.4	N17, E32	8525	β	05:43	No
1999 Jun 4.....	07:26	289	2230	-158	06:52	M3.9	N17, W69	8552	β	07:02	Yes
2000 Feb 29.....	15:30	53	1395	-72	15:15	C6.9	N22, W73	8879	β	...	No
2000 Jun 25.....	07:54	165	1617	-17	07:17	M1.9	N16, W55	9046	β	07:51	Yes
2000 Jul 10.....	21:50	289	1352	35	21:05	C6.9	N18, E49	9077	$\beta\gamma$	21:21	No
2000 Jul 14.....	10:54	Halo	1674	-96	10:03	X5.7	N22, W07	9077	$\beta\gamma\delta$	10:17	No
2000 Sep 12.....	11:54	Halo	1550	58	11:31	M1.0	S17, W09	9163	β	11:33	No
2000 Nov 8.....	23:06	170	1738	69	22:42	M7.4	N02, W77	9213	β	...	No
2000 Nov 25.....	01:31	Halo	2519	-331	00:59	M8.2	N07, E50	9240	β	01:07	Yes
2001 Jan 20.....	21:30	Halo	1507	-41	21:06	M7.7	S07, E46	9313	β	21:12	No
2001 Apr 2.....	22:06	244	2505	108	21:32	X20.0	N16, W68	9393	$\beta\gamma\delta$	21:49	No
2001 Apr 3.....	03:26	292	1613	-16	03:25	X1.2	S21, E83	9415	$\beta\gamma\delta$...	No
2001 Apr 5.....	17:06	Halo	1390	-21	16:57	M5.1	S24, E50	9415	$\beta\gamma\delta$...	Yes
2001 Apr 10.....	05:30	Halo	2411	211	05:06	X2.3	S23, W09	9415	$\beta\gamma\delta$	05:13	No
2001 Jul 19.....	10:30	166	1668	-11	09:52	M1.8	S08, W62	9537	β	...	No
2001 Aug 25.....	16:50	Halo	1433	-46	16:23	X5.3	S17, E34	9591	$\beta\gamma\delta$	16:32	No
2001 Sep 24.....	10:30	Halo	2402	54	09:32	X2.6	S16, E23	9632	$\beta\gamma\delta$...	No
2001 Oct 1.....	05:30	Halo	1405	97	04:41	M9.1	S18, W83	9628	$\beta\gamma$...	No
2001 Oct 22.....	15:06	Halo	1336	-8	14:27	M6.7	S21, E18	9672	β	14:52	No
2001 Nov 4.....	16:35	Halo	1810	-63	16:04	X1.0	N06, W18	9684	$\beta\gamma$	16:10	No
2001 Nov 17.....	05:30	Halo	1379	-22	04:49	M2.8	S13, E42	9704	$\beta\gamma\delta$	05:00	No
2001 Nov 22.....	20:30	Halo	1443	-43	20:18	M3.8	S25, W67	9698	β	20:22	Yes
2001 Nov 22.....	23:30	Halo	1437	-12	22:32	M9.9	S17, W37	9704	β	22:31	No
2001 Dec 26.....	05:30	212	1446	-39	04:32	M7.1	N08, W54	9742	$\beta\gamma$	04:59	Yes
2002 Apr 21.....	01:27	256	2409	16	00:43	X1.5	S14, W84	9906	$\beta\gamma$	01:18	Yes
2002 May 22.....	03:50	Halo	1494	0	03:18	C5.0	S20, W72	9948	α	...	Yes
2002 Jul 23.....	01:31	Halo	1726	-190	00:18	X4.8	S13, E72	0039	β	00:28	Yes
2002 Aug 14.....	02:30	133	1309	-28	01:47	M2.3	N09, W54	0061	β	01:57	Yes
2002 Aug 16.....	06:06	152	1316	-14	05:46	M2.4	N07, W87	0061	β	05:52	Yes
2002 Aug 16.....	12:30	Halo	1459	-25	11:32	M5.2	S14, E20	0069	$\beta\gamma\delta$	11:41	No
2002 Aug 24.....	01:27	Halo	1878	-21	00:49	X3.1	S02, W81	0069	$\beta\gamma\delta$	01:01	Yes
2002 Nov 9.....	13:31	Halo	1838	35	13:08	M4.6	S12, W29	0180	$\beta\gamma\delta$	13:17	No
2002 Nov 10.....	03:30	Halo	1516	-126	03:04	M2.4	S12, W37	0180	$\beta\gamma\delta$	03:14	Yes

^a Indicates the first appearance time in the LASCO C2 field of view.

^b Indicates the representative speed in the LASCO C2 and C3 fields of view.

^c Indicates the acceleration from second-order fit.

Cane et al. (2000) showed that only about half of front-side halo CMEs encountered the Earth, and their associated solar events typically occurred from 40° east to 40° west in longitude. According to Wang et al. (2002), about 45% of the total 132 Earth-directed halo CMEs caused geomagnetic storms with $K_p \geq 5$, and almost 83% of events took place within $\pm 30^\circ$ of the central meridian. Even though the halo CMEs that originated from the central meridian are the best candidate for geoeffective CMEs, we note that still some fraction of such CMEs were non-geoeffective and some CMEs produced only weak geomagnetic storms. Thus, we may ask, what kinds of CME physical characteristics are associated with “control” of their geoeffectiveness? For this objective, we examine the relation between quantitative physical parameters of 12 front-side halo CMEs (whose longitudes are within 40° of central meridian) and the Dst index. In this study, we consider the column density of a CME, its total mass, the location of its associated flare and its “direction.” To quantify the CME direction, we propose a new direction parameter that is directly estimated from coronagraph observations. To

our knowledge, our approach is the first trial on the quantitative comparison between the CME direction (or density) and geomagnetic activity.

In § 2, we explain our data analysis and event selection procedure. We present the associations of these very fast CMEs with other solar activities as well as the correlation between front-side halo CMEs near the central meridian and the Dst index in § 3. A brief summary and conclusion are delivered in § 4.

2. DATA AND EVENT SELECTION

The LASCO C2 instrument is an externally occulted white light coronagraph that observes Thomson-scattered visible light through a broadband filter. It covers 2–6 R_\odot with a pixel resolution of 12"1 (Brueckner et al. 1995). The height-time data of the CMEs used in this study are taken from the online *SOHO* LASCO CME catalog⁶ in which CME kinematics are estimated and compiled from LASCO C2 and C3 images. The EUV Imaging

⁶ See http://cdaw.gsfc.nasa.gov/CME_list/.

Telescope (EIT) provides spectroheliograms of the corona and transition region on the solar disk and up to $1.5 R_{\odot}$ above the solar limb. It allows us to diagnose solar plasma at certain temperatures in the range of 6×10^4 to 3×10^6 K (Delaboudiniere et al. 1995). The time cadence of the EIT images used in this study is a few tens of minutes, and their pixel resolution is about $2''6$.

We consider the *SOHO* LASCO CMEs (1996–2002) whose speeds are larger than 1300 km s^{-1} from the *SOHO* LASCO online catalog. Then we inspected all EIT and LASCO images of these events, as well as their running difference images, to identify whether they are front-side events and whether the CMEs are associated with flares. The main criterion is whether EIT brightenings and/or EIT dimmings are coincident spatially and temporally with the eruption of a LASCO CME. The solar surface locations of the associated solar flares are taken from the National Geophysical Data Center (NGDC).⁷ The locations were also independently confirmed from brightenings in EIT images. Finally, we chose 38 very fast front-side CMEs whose basic information (LASCO C2 appearance time, width, linear-fit speed, and acceleration) is summarized in Table 1. On the other hand, we inspected the LASCO images of all 38 front-side CMEs to check whether they look like broad CMEs due to shock deflections (Sheeley et al. 2000), as suggested by Zhao (2005). We also examined the associations of these CMEs with solar type II radio bursts whose information is archived by NGDC.⁸

For further detailed examination on the CME geoeffectiveness, we selected 12 halo CMEs whose longitudes are less than 40° . These CMEs are thought to be the most plausible candidates of geoeffective CMEs from previous studies (e.g., Cane et al. 2000; Wang et al. 2002). Then we identified their association with ICMEs and geomagnetic storms characterized by Dst indices using two comprehensive catalogs of Cane & Richardson (2003) and Cho et al. (2003). For the events whose information is not available, we used Dst indices⁹ that are assumed to be local minimum values within a 15–72 hr window after the CME initiation.

3. PHYSICAL PARAMETERS

3.1. Mass and Column Density

It is well accepted that white light brightenings (e.g., CMEs) seen in coronagraph images come from the photospheric light scattered by coronal electrons. Based on this fact, it is possible to compute the coronal mass and column density of a CME in a conventional way (Poland et al. 1981; Vourlidas et al. 2000). Our procedure is as follows: (1) selected LASCO images are calibrated in units of solar brightness; (2) a suitable pre-event image without any CME is subtracted from each of the CME images; (3) the region of interest is selected by visual inspection of the pre-event subtracted images; (4) the number of electrons is simply the ratio of the observed brightness B_{obs} over the brightness $B_e(\theta = 0)$ of a single electron at some angle θ from the plane of sky, where $B_e(\theta)$ is the Thomson scattering function; (5) the mass per unit pixel is then calculated as follows:

$$m(x, y) = \frac{B_{\text{obs}}(x, y)}{B_e(\theta)} (1.97 \times 10^{-24}) \text{ g}, \quad (1)$$

where the ejected material is assumed to be composed of a mix of completely ionized hydrogen and 10% helium; (6) the column

density (g cm^{-2}) is directly calculated from $m(x, y)$ by considering the pixel size of a CCD; and (7) the total mass (in g) is finally obtained by integrating $m(x, y)$ over the region of interest and the mean column density is also derived. Practically, we used Solarsoft¹⁰ IDL (Interactive Data Language) routines (e.g., *cme_mass.pro*) for our calculations. To minimize the dependence of the CME mass and density on the distance from solar center, we used the LASCO C3 data whose location is the nearest from $20 R_{\odot}$. Some detailed discussions on the accuracy of the mass calculation and the errors are well described by Vourlidas et al. (2000).

3.2. Location and Direction Parameter

It is well known that a significant fraction of halo CMEs are geoeffective. According to previous studies (Cane et al. 2000; Wang et al. 2002), only about 50% of all halo CMEs are geoeffective, and the others are not. In addition, most of the geoeffective halo CMEs originated near the central meridian when the locations of their associated flares are used. Thus, we may suppose that halo CMEs that originated near the central meridian have higher possibilities of causing strong geomagnetic storms. In this case, the location of the associated flare can be a geoeffective parameter as originally suggested by Haurwitz et al. (1965). Our location parameter is defined as the directional cosine ($\cos \theta$) between the associated flare location and solar disk center.

Here we note that the location parameter may not properly indicate the central axis of the ICME's propagation direction—at least in some cases. As a more direct parameter, we propose a direction parameter that can be directly available from coronagraph observations. Let us consider the shape of two halo CMEs, as shown in Figure 1. If the front of a CME is directly propagating toward the Earth, the shape in its pre-event subtracted image should be nearly symmetric (like a circle) as shown in the left panel of Figure 1. If the front of a CME is propagating away from the Sun–Earth line, its shape should be quite asymmetric, as seen in the right panel of Figure 1.

To quantify its symmetric characteristics, we suggest a quantitative parameter as follows: (1) a pre-event image is subtracted, (2) an ellipse is plotted on the image and then its major and minor axes are manually adjusted in such a way that the ellipse can approximately follow the front edge of a CME, (3) straight lines connecting pairs of opposite positions on the CME front are considered, (4) the ratio (b/a) between the shorter distance (b) from the solar disk center and the longer distance (a) is obtained, and (5) its maximum value is finally estimated as the direction parameter; equivalently, the line having the maximum ratio corresponds to an extension of the line connecting solar center and the center of the ellipse. Geometrically, the proposed parameter depends on the ratio of the distance between the ellipse center and solar center to the distance between the center of the ellipse and the CME front. While the direction parameter ($DP = b/a$) of the 2000 July 14 event (*left*) of Figure 1 is 0.64, the parameter of the 2000 September 12 event (*right*) is 0.32. This fact implies that the first event is more symmetric than the second one; that is, the direction of the first event is more oriented toward the Earth. In fact, while the first CME is associated with a very strong geomagnetic storm ($Dst = -300 \text{ nT}$), the second CME did not produce any remarkable geomagnetic activity.

4. RESULTS

Statistical results of the very fast CMEs are summarized in Table 1. We found that among 38 front-side fast CMEs, 25 are

⁷ See <http://www.ngdc.noaa.gov/stp/SOLAR/ftpsolarflares.html>.

⁸ See <http://www.ngdc.noaa.gov/stp/SOLAR/ftpsolarradio.html>.

⁹ See <http://spidr.ngdc.noaa.gov/spidr/>.

¹⁰ See <http://sohowww.nascom.nasa.gov/solarsoft/>.

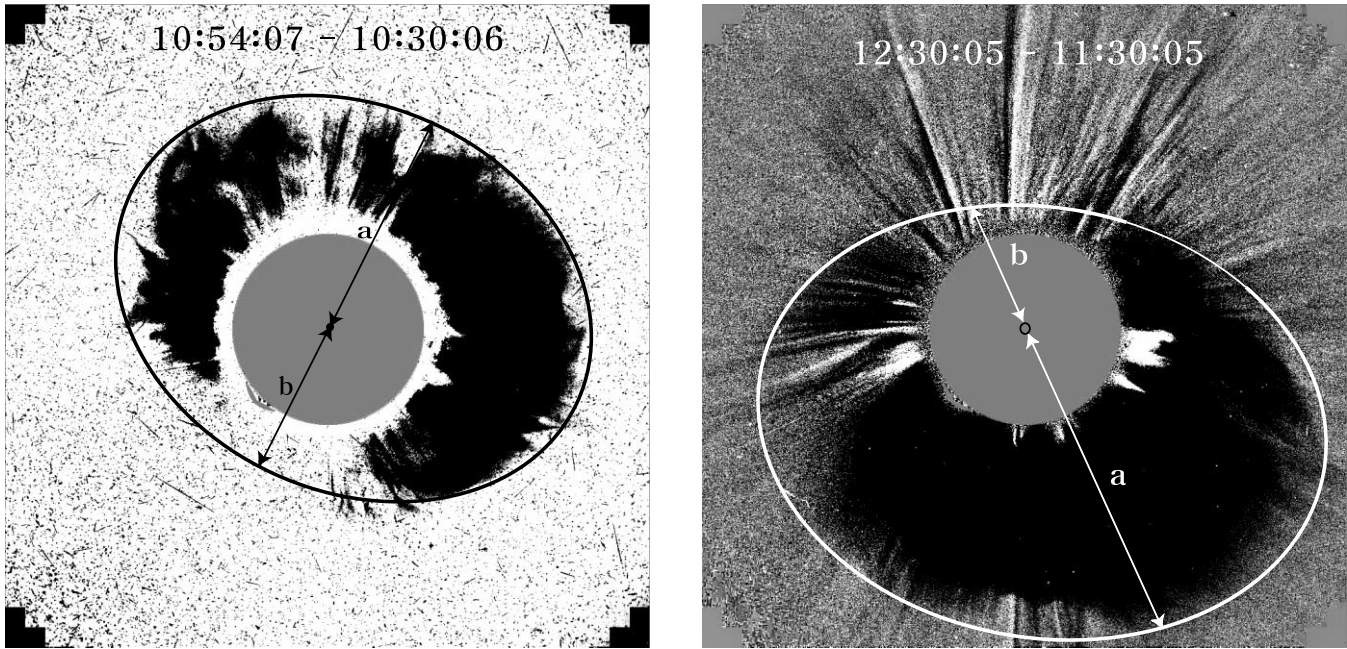


FIG. 1.—LASCO C2 running difference images of the 2000 July 14 event (*left*) and the 2000 September 12 event (*right*). How to estimate a and b is described in text.

halo (or full halo) CMEs with span of 360° , 12 are partial halo CMEs with span greater than 130° , and only one is a broadside CME with a span of 53° (2000 February 29 event). There are 13 events that are shock-deflected CMEs: six are full halo CMEs and seven are partial halo CMEs. All the CMEs are associated with X-ray flares (X-12, M-23, C-3), and most of them (35/38) are accompanied by major flares such as X and M class. This is consistent with the kinematic tendency of two types of CMEs (Andrews & Howard 2001; Moon et al. 2002). Table 1 shows 31 CME-associated active regions, most of which have bipolar (β) type or more complex magnetic configurations, such as $\beta\gamma$ or $\beta\gamma\delta$ type. Thus, we expect that they have relatively large magnetic free energy as well as strong MHD forces that could produce very fast CMEs. Moreover, the bias of these fast CMEs in the direction of the Archimedian interplanetary magnetic field (IMF) spiral suggests that there existed an early, near-Sun, net Lorentz force in that direction (see also Wei & Dryer [1991], who suggested a Lorentz force component also in the direction of the heliospheric current sheet). For about 80% of the events (33/38), type II bursts were reported as coronal shock signatures. These results show that very fast coronal CMEs are intimately associated with other major solar activities, such as major X-ray flares and type II bursts.

Figure 2 shows the longitudinal distribution of the flares associated with the very fast CMEs. As seen in the figure, the distribution is rather asymmetric; about 60% (23/38) of all CMEs originated from the western hemisphere, which is similar to the results obtained by Wang et al. (2002), who studied halo CMEs from 1997 to 2000. It is also noted that about one-third (13/38) of the events originated near the west limb ($\geq W60^\circ$), which is about 2 times larger than the probability from equal distribution. Such a distribution seems to be caused by both the fact that a CME that originated from the limb is likely to be much less affected by the projection effect and the fact that a CME trajectory from the west limb is much less deflected by the solar rotation. Noting that we did not select broad CMEs but very fast CMEs whose speeds are larger than 1300 km s^{-1} , we expect that limb CMEs are more favorably selected than disk CMEs. It

is also found that about one-third of the events (13/38) were strongly affected by shock deflections, and most of them originated near the limb.

For the further examination of CME geoeffectiveness, we selected 12 CMEs whose longitudes are within 40° of central meridian. Table 2 shows their physical parameters and their associations with ICMEs and geomagnetic storms. Figure 3 shows the CME total mass versus the absolute value of the Dst index and the CME mean column density versus the absolute value of Dst index. It is found that while the CME total mass has a poor correlation with the Dst index, the CME column density has a much better correlation with the Dst index. To quantify the relationship, we estimated Spearman rank-order correlation coefficients (r_s) between considered CME parameters and Dst index, and the two-sided significance levels (P) of their deviations from zero. A small value of P indicates a significant correlation or anticorrelation. The estimated correlation values and their significance levels are as follows: $r_s = 0.67$ and $P = 0.017$ for the CME

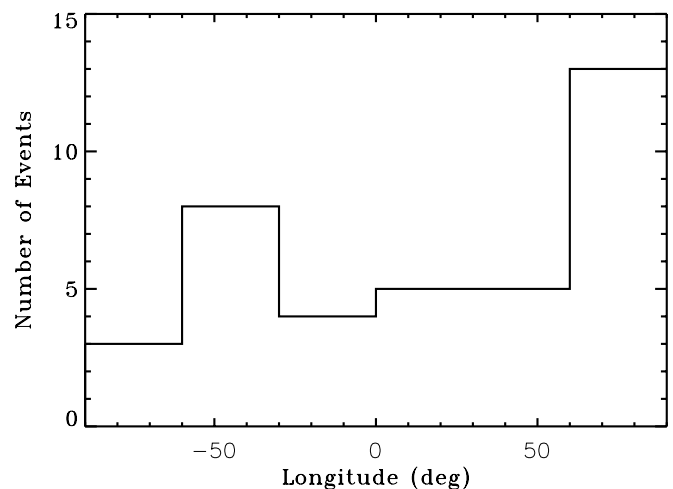


FIG. 2.—Longitudinal distribution of the 38 flares associated with very fast CMEs.

TABLE 2
PHYSICAL CHARACTERISTICS OF THE CMEs AND THEIR GEOEFFECTIVENESS

Date	Time	Mass (M) (10^{15} g)	Density (ρ) (10^{10} g cm $^{-2}$)	θ^a (deg)	DP b (b/a)	CP c $\rho(b/a)$	ICME d Start	Dst (min)
1998 Apr 29.....	16:58	10	8.9	27	0.47	4.20	May 2 05:00	-100
1999 May 3.....	06:06	9.3	5.9	36	0.19	1.10	...	-20
2000 Jul 14.....	10:54	32	37	23	0.64	23.7	Jul 15 19:00	-300
2000 Sep 12.....	11:54	20	13.0	19	0.32	4.16	...	-40
2001 Apr 10.....	05:30	12	12.0	25	0.61	7.32	Apr 11 22:00	-257
2001 Aug 25.....	16:50	8.4	6.4	38	0.16	1.02	...	-20
2001 Sep 24.....	10:30	14	11.7	28	0.32	3.74	Sep 25 24:00	-100
2001 Oct 22.....	15:06	12	6.4	27	0.38	2.43	...	-76
2001 Nov 4.....	16:35	19	18	19	0.59	10.62	Nov 6 02:00	-277
2001 Nov 22.....	23:30	16	13	40	0.50	6.50	Nov 24 14:00	-200
2002 Aug 16.....	12:30	13	9.1	24	0.40	3.64	Aug 19 12:00	-50
2002 Nov 9.....	13:31	6.4	4.4	31	0.24	1.06	...	-23

^a Indicates the angular distance of the associated flare location from the solar disk center.

^b Indicates the new CME direction parameter.

^c Indicates the combined parameter: CME column density times b/a .

^d Indicates the arrival time of the ICME (Cane & Richardson 2003), in month, day, and hour.

total mass and $r_s = 0.80$ and $P = 0.002$ for the CME column density. Since the column density of a CME is an integrated mass per unit area along the line of sight, it can be affected by its mass density as well as its direction.

Figure 4 shows the location parameter ($\cos \theta$) versus the Dst index and the new direction parameter DP(b/a) versus the Dst index. Those two parameters were well described in the last section. It is found that while the location parameter does not have a good relationship with the Dst index, the direction parameter, DP, of a CME has quite a good correlation with the Dst index. The estimated Spearman rank-order correlation values and their significance levels are as follows: $r_s = 0.48$ and $P = 0.114$ for $\cos \theta$ and $r_s = 0.93$ and $P = 1.2 \times 10^{-5}$ for the proposed direction parameter. In contrast, our new direction parameter is quite promising in that it well represents the direction of a CME in the sense of a geometrical concept, as well as in that it has a much better relationship with the Dst index than any other parameters under consideration. On the other hand, our results imply that the location of the associated flare does not accurately reflect its direction to the Earth, at least in some cases. In a strict sense, the location can be used as a direction parameter both when the source region of a halo CME corresponds to the location of its associated flare and when the halo CME is radially ejected from the source region. In this sense, the proposed direction parameter is thought to be more meaningful.

We also examined several other parameters, such as the CME's associated flare strength, its speed, its dynamic pressure, and its kinetic energy, but we failed to obtain good results. Our preliminary investigations of the magnetic field orientation of CME-producing active regions based on the coronal flux rope model are not conclusive.

5. SUMMARY AND DISCUSSION

In this paper, we examine the physical characteristics of very fast CMEs whose speeds in the *SOHO* LASCO field of view are larger than 1300 km s $^{-1}$. By carefully examining all *SOHO* EIT and *SOHO* LASCO images of the CMEs, we selected 38 front-side CMEs. Then we examined their associations with other solar activities. Main results can be summarized as follows. First, about two-thirds (25/38) of these fast CMEs are halo CMEs. Second, about 60% of the CMEs were ejected from the western hemisphere. Third, all the CMEs are associated with X-ray flares that are stronger than C5 class, and about one-third is associated with X-class flares. Fourth, about 80% of the CMEs were accompanied by type II radio bursts as coronal shock signatures. Fifth, about one-third of the events (13/38) were strongly affected by shock deflections, and most of them originated near the limb.

For the examination of CME geoeffectiveness, we selected 12 halo CMEs whose longitudes are less than 40° , which are thought to be the most plausible candidates for geoeffective CMEs. For

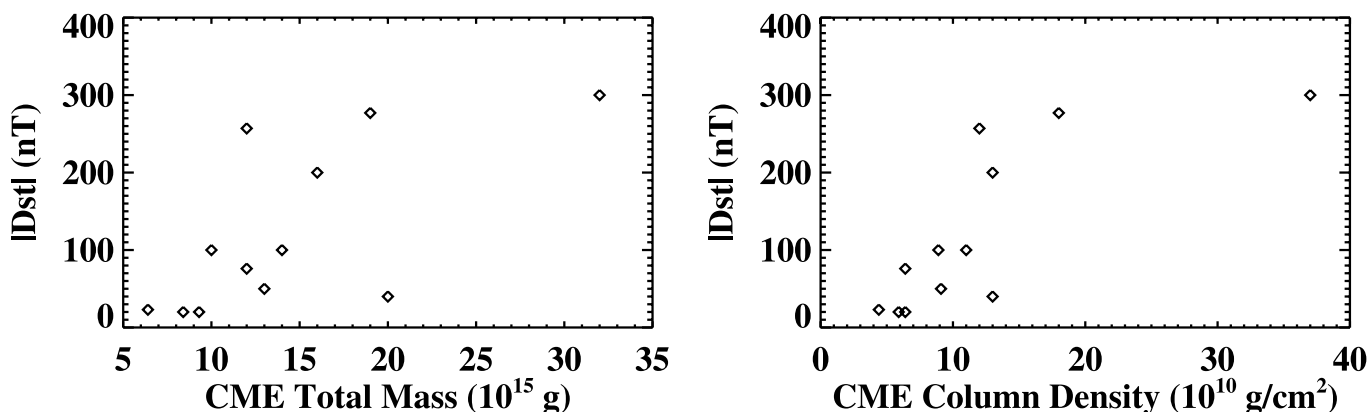


FIG. 3.—CME mass vs. Dst index (left) and CME mean column density vs. Dst index (right).

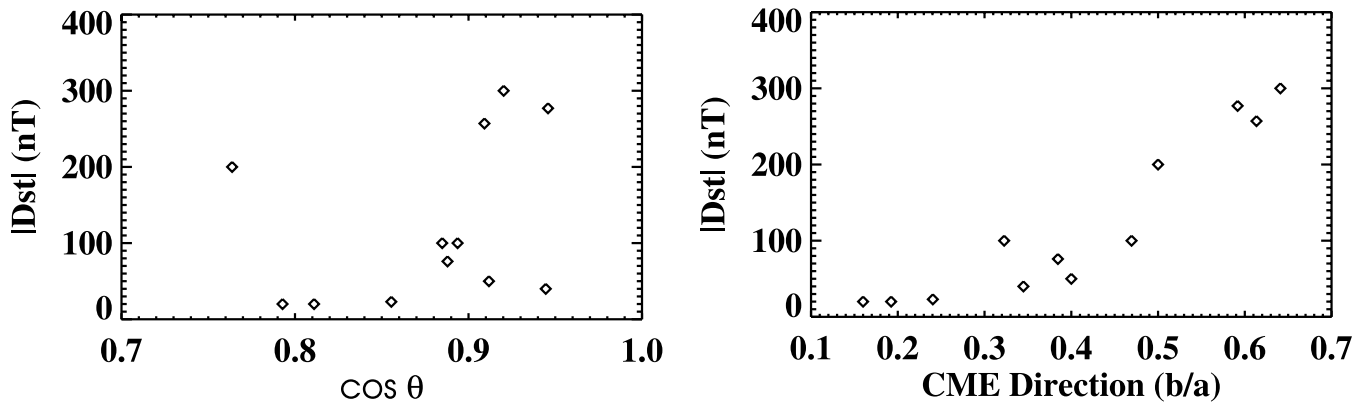


FIG. 4.—Location parameter ($\cos \theta$) vs. Dst index (*left*) and direction parameter ($DP = b/a$) vs. Dst index (*right*).

these 12 events, we examined the relationship between their CME physical parameters and the Dst index. In particular, a direction parameter is proposed as a new geoeffective parameter. Its main advantages are that it can be directly estimated from coronagraph observation, as well as that it is well understood as a geometrical concept. It is found that while the flare location has a poor correlation with the Dst index, the new direction parameter has a quite good correlation. We also found that the column density of a CME also has a comparably good correlation with the Dst index. We note that the CME column density is strongly affected by the direction of a CME in addition to its mass density, since it is an integrated density along the line of sight. Thus, we conclude that the direction is a quite important parameter that controls the CME geoeffectiveness. It is also noted that several other parameters, such as the CME's associated flare strength, speed, dynamic pressure, and kinetic energy, are not so geoeffective. Considering that an ICME is probably an interplanetary expansion of coronal flux rope, we expect that the CME density is well correlated to the density of its associated ICME, which may be a reason why we have a good correlation between the CME column density and the Dst index. In the case of CME speed, we did not obtain good results, which differs from Srivastava & Venkatakrishnan (2002),

who showed a possible relationship using five geoeffective CMEs. In summary, our results show a good possibility that the CME direction and density, which are directly estimated from coronagraph observations, are important physical parameters that control the geoeffectiveness of very fast halo CMEs. More extensive investigations on several physical parameters using all halo CME-Dst pairs from 1997 to 2003 are in preparation.

The authors greatly appreciate the referee's constructive comments. This work has been supported by the MOST grants (M1-0104-00-0059, M1-0336-00-0011, M1-0336-00-0013, and M1-0407-00-0001) of the Korean government. M. D. was supported by NASA's Living with a Star program via grant NAG5-12527 to Exploration Physics International, Inc. M. D. also thanks NOAA's Space Environment Center for their hospitality. The CME catalog we have used is generated and maintained by the Center for Solar Physics and Space Weather, The Catholic University of America in cooperation with the Naval Research Laboratory and NASA. *SOHO* is a project of international cooperation between ESA and NASA.

REFERENCES

- Andrews, M. D. 2003, *Sol. Phys.*, 218, 261
 Andrews, M. D., & Howard, R. A. 2001, *Space Sci. Rev.*, 95, 147
 Brueckner, G. E., et al. 1995, *Sol. Phys.*, 162, 357
 Cane, H. V., & Richardson, I. G. 2003, *J. Geophys. Res.*, 108, 6
 Cane, H. V., Richardson, I. G., & St. Cyr, O. C. 2000, *Geophys. Res. Lett.*, 27, 3591
 Cho, K.-S., Moon, Y.-J., Dryer, M., Fry, C. D., Park, Y. D., & Kim, K.-S. 2003, *J. Geophys. Res.*, 108, 8
 Delaboudiniere, J.-P., et al. 1995, *Sol. Phys.*, 162, 291
 Dryer, M. 1994, *Space Sci. Rev.*, 67, 363
 Gallagher, P. T., Lawrence, G. R., & Dennis, B. R. 2003, *ApJ*, 588, L53
 Haurwitz, N. W., Yoshida, S., & Akasofu, S.-I. 1965, *J. Geophys. Res.*, 70, 2977
 MacQueen, R. M., & Fisher, R. R. 1983, *Sol. Phys.*, 89, 89
 Maia, D., Vourlidas, A., Pick, M., Howard, R., Schwenn, R., & Magalhães, A. 1999, *J. Geophys. Res.*, 104, 12507
 Moon, Y.-J., Cho, K.-S., Smith, Z., Fry, C. D., Dryer, M., & Park, Y. D. 2004, *ApJ*, 615, 1011
 Moon, Y.-J., Choe, G. S., Wang, H., Park, Y. D., Gopalswamy, N., Yang, G., & Yashiro, S. 2002, *ApJ*, 581, 694
 Poland, A. I., Howard, R. A., Koomen, M. J., Michels, D. J., & Sheeley, N. R., Jr. 1981, *Sol. Phys.*, 69, 169
 Raymond, J. C., Ciaravella, A., Dobrzycka, D., Strachan, L., Ko, Y.-K., Uzzo, M., & Rauaafi, N.-E. 2003, *ApJ*, 597, 1106
 Sheeley, N. R., Jr., Hakala, W. N., & Wang, Y.-M. 2000, *J. Geophys. Res.*, 105, 5081
 Sheeley, N. R., Jr., Walters, J. H., Wang, Y.-M., & Howard, R. A. 1999, *J. Geophys. Res.*, 104, 24739
 Srivastava, M., & Venkatakrishnan, P. 2002, *Geophys. Res. Lett.*, 29, 1
 St. Cyr, O. C., Burkepile, J. T., Hundhausen, A. J., & Lecinski, A. R. 1999, *J. Geophys. Res.*, 104, 12493
 St. Cyr, O. C., et al. 2000, *J. Geophys. Res.*, 105, 18169
 Vourlidas, A., Subramanian, P., Dere, K. P., & Howard, R. 2000, *ApJ*, 534, 456
 Wang, Y. M., Ye, P. Z., Wang, S., Zhou, G. P., & Wang, J. X. 2002, *J. Geophys. Res.*, 107, 2
 Wei, F.-S., & Dryer, M. 1991, *Sol. Phys.*, 132, 373
 Zhang, J., Dere, K. P., Howard, R. A., & Bothmer, V. 2003, *ApJ*, 582, 520
 Zhao, X. P. 1992, *J. Geophys. Res.*, 97, 15051
 ———. 2005, in *IAU Symp. 223, Multi-Wavelength Investigations of Solar Activity*, ed. A. V. Stepanov, E. E. Benevolenskaya, & A. G. Kosovichev (Cambridge: Cambridge Univ. Press), in press
 Zhao, X. P., & Webb, D. F. 2003, *J. Geophys. Res.*, 108, 4